Studies on Blends of Binary Crystalline Polymers. 1. Miscibility and Crystallization Behavior in Poly(butylene terephthalate)/Polyarylates Based on Bisphenol A Isophthalate

A. S. Liu, W. B. Liau,* and W. Y. Chiu

Institute of Materials Science and Engineering, National Taiwan University, Taipei, 106, Taiwan, Republic of China

Received March 26, 1998; Revised Manuscript Received July 9, 1998

ABSTRACT: The miscibility and crystallization behavior of binary crystalline blends of poly(butylene terephthalate) [PBT] and polyarylate based on Bisphenol A isophthalate [PAr(I-100)] have been investigated using differential scanning calorimetry (DSC) and wide-angle X-ray diffraction (WAXD). Both polymers were able to crystallize over a wide range of blend composition and temperature. This blend system exhibited a single composition-dependent glass-transition temperature over the entire composition range and two distinctive melting peaks in some compositions. The equilibrium melting point depressions of both PBT and PAr(I-100) were observed, and the Flory−Huggin's interaction parameter of $\chi_{12(PBT)} = -1.3$ was obtained. It indicated that these blends were thermodynamically miscible in the melt. The crystallization rate of neat PAr(I-100) was very slow. However, it was much faster when the PBT was added. The crystallization rate of PAr(I-100) was significantly influenced when the PBT crystal was previously formed. It was not only due to the amorphous phase composition shifted to a richer PAr(I-100) content after the crystallization of PBT but also to the constraint of the PBT crystal phase. On the other hand, the crystallization rate of PBT was reduced due to the addition of PAr(I-100).

Introduction

In the past two decades, many miscible polymer blends have been well studied and documented by industrial and scientific research.[1,2] Most of them focused on the polymeric mixture containing two amorphous components or amorphous and semicrystalline components.[3−5] On the other hand, polymer blends containing two crystalline components are less frequently discussed.

In crystalline/crystalline blends, cocrystallization is unfavorable because it requires close matching of chain conformations and lattice parameters. Furthermore, both polymers must exhibit a certain degree of miscibility in the melt and the crystallization kinetics of both polymers cannot be significantly different, as has been discussed and issued by Kyu and Vadhar.[6] However, only a few cases are identified as isomorphic systems.[7−9] For example, the study of a poly(aryl ether ketone) blend has proven to be the cocrystallization since the difference of the ketone content is less than 25 wt %.[10] More recently, several blends such as poly(ethylene oxide)/poly(3-hydroxybutyrate),[11] poly(vinylidene fluoride)/poly(3-hydroxybutyrate),[12] poly(vinylidene fluoride)/poly(1,4-butylene adipate),[13] and poly(ethylene terephthalte)/poly(butylene terephthalte)[14] have been studied and reported in the literature.

The purpose of the present study is to understand the nature of miscibility and crystallization behavior in crystalline/crystalline polymer blends. In this work, we tentatively chose the poly(butylene terephthalate) [PBT] and polyarylates [PAr(I-100)], a homopolymer of Bisphenol A isophthalate, as the blend system. These polymers are both crystalline in their neat state, which undergo crystallization over a wide range of temperature. Nevertheless, the melting point of PBT is ca. 224 °C and that of PAr(I-100) is ca. 300 °C. Therefore, the crystallization behaviors of both components can be studied separately due to the more than 70 °C difference in melting point.

Polyarylates based on Bisphenol A with isophthalates are not commercially available now. However, its homologous copolymers (i.e., polyarylates based on Bisphenol A with iso/terephthalates), PAr have been commercialized and recognized as important materials due to high distortion temperature, excellent mechanical properties, and toughness, especially the ultraviolet (UV) resistance after long time exposure.[15−17] The polymer blends of PBT and commercialized PAr have been studied intensively.[18−20] However, the study of PBT/PAr(I-100) blends is limited. According to their studies, PBT/PAr blends were shown to be miscible by precipitation from 40:60 wt % tetrachloroethane/phenol−methanol. Hence, it is expected that the PBT/PAr(I-100) is a miscible blend. An intermediate can be obtained with properties to meet certain needs. Most of all, the concepts to explain the binary crystalline phenomenon of PBT/PAr(I-100) are somewhat different compared with the traditional viewpoints.

Experimental Section

Materials. The PBT sample was kindly supplied by Nan-Ya Plastics Co. Inc. (article no. PBT-1100). Its intrinsic viscosity (IV) was ca. 0.85 dL/g, determined from 60:40 wt % phenol/1,1,2,2-tetrachloroethane cosolvent at 30°C. The M_n of PBT was converted from IV to be 27 400 by using an adequate Mark−Houwink constant.[21] The PAr(I-100) used in this work was synthesized by feeding Bisphenol A with 100% isophthaloyl chloride via interfacial polymerization. The PAr-(I-100) was a homopolymer of polyarylate. The detailed preparation and reaction mechanism were demonstrated in Chu and Lee's[22] work. Its weight-averaged molecular weight ($M_w \sim 61\,400$) was measured by gel-permeation chromatog-

* To whom all correspondence should be addressed. Tel: 886-2-2362-6119. Fax: 886-2-2363-4562. E-mail: wbliau@ccms.ntu.edu.tw.

S0024-9297(98)00487-2 CCC: $15.00
Published on Web 09/03/1998

raphy (GPC) in tetrahydrofuran solution relative to polystyrene standards.

Blends of PBT and PAr(I-100) were prepared by dissolving a total amount of 2 g of PBT/PAr(I-100) in weight fractions 100/0, 85/15, 65/35, 50/50, 35/65, 15/85, and 0/100 in 100 mL of the same cosolvent, as described in intrinsic viscosity measurements. Stock solutions of both polymers were stirred at 80 °C for 4 h and then dropwise added to ten-fold excess of methanol. To remove the residual solvent completely, the precipitate was filtered off and washed with methanol. Then the resulting precipitate was further placed in vacuum oven at 100 °C for 3 days until it reached constant weight. To make sure that the solvent was removed completely, it was checked by TGA. The result of TGA did not show any weight loss before 300 °C.

Characterization. The backbone structure of PAr(I-100) was checked by the ^{1}H-NMR technique. These detailed procedures could be found in the literature reported by Runt et al.[23] The NMR results showed that the polymer was a homopolymer of polyarylate. The measurement of the thermal behavior was conducted with a DuPont TA instruments (DSC 9900) equipped with a liquid nitrogen cooling system. The corresponding peak temperature and heat of fusion were calibrated using pure indium and cadmium standards. Sealed aluminum pans containing 5−10 mg samples were operated at the scanning rate of 20 °C/min in all experiments. In order to eliminate the previous thermal history, all samples were heated above the melting point (i.e., 300 °C) for 5 min so as to destroy the initial morphology. For the determination of glass-transition temperatures, the cell must be cooled as quickly as possible. The glass-transition temperature was recorded as the midpoint of heat capacity jump, and the melting point was obtained from the peak value of the endotherm from the second run. All measured data reported are at least twice those of DSC scans based on mean values. Wide-angle X-ray diffraction (WAXD) was performed on a Philips PW-1170 rotating anode generator with nickel-filtered Cu Kα radiation at an accelerating voltage of 40 kV and a current of 30 mA. The samples used in WAXD were prepared by compression molding. The sample thickness was approximately 0.2 mm. Data were collected with a step size of 0.04° from $2\theta = 10$ to 60°. The calibration of sample-to-detector distance was employed using the silicon single crystal.

Results and Discussion

The glass-transition temperature (T_g) was measured on the melt-quenched samples of PBT/PAr(I-100) at a cooling rate over 100 °C/min and a heating rate of 20 °C/min. The glass-transition temperatures of blends observed in dynamic DSC scans were indicated by an arrow in Figure 1. A single composition-dependent T_g with intermediate value between their respective neat state was found for each blend. It indicated that PBT and PAr(I-100) were miscible in the melt. The partial crystallization of PBT was inevitable even partial crystallization of PBT under such quickly quenching conditions, except for the blends that the PBT weight ratio was less than 65 wt % (Figure 1 and Table 1). On the other hand, PAr(I-100) partially crystallized for the blends of PBT/PAr(I-100) = 35/65 and 15/85 on quenching process (Figure 1 and Table 1). The amorphous composition must be corrected due to the crystallization during the quenching process. The crystallinity of PBT ($\chi_{c,PBT}$) in melt-quenched sample was calculated from the following equation:

$$\chi_{c,PBT} = \frac{\Delta H_{m,PBT} - \Delta H_{c,PBT}}{\Delta H^{\circ}_{f,BPT}}$$

where $\Delta H_{c,PBT}$ was the recrystallization exotherm, $\Delta H_{m,PBT}$ was the melting endotherm of PBT, and

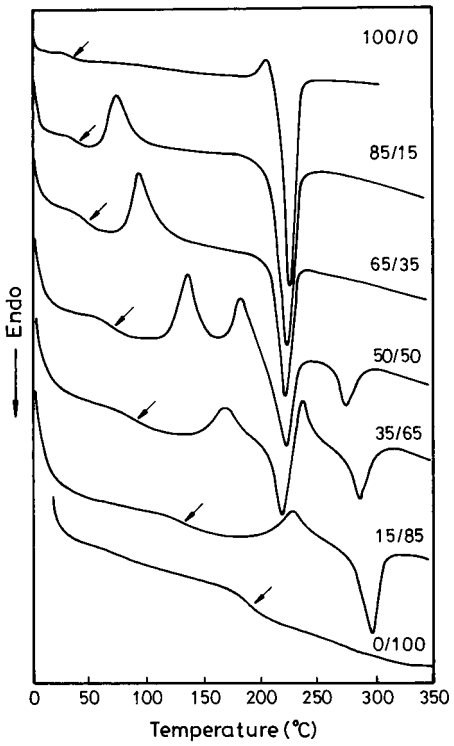

Figure 1. DSC traces recorded from second run of PBT/PAr-(I-100) Blends. T_g is indicated by an arrow.

$\Delta H^{\circ}_{f,BPT}$ was the fusion heat of 100% PBT crystal. Then, the composition of amorphous was calibrated by removing these previously formed PBT crystalline fractions. The crystallinity of PAr(I-100) in the melt-quenched sample was not able to be calculated due to the lack of the heat of fusion of 100% PAr(I-100) crystal. However, the crystallization of PAr(I-100) during quenching was so slight that the correction of amorphous composition was not necessary, except for blends of PBT/PAr(I-100) = 35/65 and 15/85. In order to be more careful in dealing with the uncorrected blends, T_g's of PBT/PAr(I-100) = 35/65 and 15/85 were not included in the following mathematical treatment of T_g's. The dependence of T_g on blend composition can be estimated using classical Fox's law,[24] (1), or Gordon−Taylor's equation,[25] (2):

$$\frac{1}{T_{g,blend}} = \frac{w_1}{T_{g,1}} + \frac{w_2}{T_{g,2}} \quad (1)$$

$$T_{g,blend} = \frac{w_1 T_{g,1} + k(1 - w_1) T_{g,2}}{w_1 + k(1 - w_1)} \quad (2)$$

where w_i is the weight fraction, k is the fitting parameter that equals $\Delta\alpha_1/\Delta\alpha_2$, and $\Delta\alpha_i$ is the difference between the volume expansion coefficients in the glassy and liquid states. $T_{g,i}$ is the glass-transition temperature of the pure component. Subscripts 1 and 2 denote the PBT and PAr(I-100), respectively. The glass transition temperature of PBT between 30 and 45 °C has been reported from DSC[18,26] measurements, which are independent of crystallinity, as described by Illers.[27] However, the T_g of PBT was influenced by the thermal lag of the instrument, which depends on the heating rate and sample mass.[27] The T_g of pure amorphous PBT seems unavailable due to the crystallization of PBT on quenching. Therefore, only four data points (85/15, 65/

Table 1. Exo/Endothermic Heats Calculation of PBT/PAr(I-100) Blends

PBT/PAr(I-100) wt fraction (%)	amorphous T_g (°C)	PBT phase			PAr (I-100) phase		
		$\Delta H_c/\Delta H_m$[a]	$\Delta H_m - \Delta H_c$[b]	ΔH_m/wt %[c]	$\Delta H_c/\Delta H_m$[a]	$\Delta H_c - \Delta H_m$[b]	ΔH_m/wt %[c]
100/0	37.87	0.05	54.48	57.46	N .A.[d]	N.A.	N.A.
85/15	43.23	0.48	27.85	63.60	N.A.	N.A.	N.A.
65/35	54.28	0.45	17.90	50.08	N.A.	N.A.	N.A.
50/50	75.36	0.98	0.56	47.66	0.98	0.17	17.07
35/65	96.60	1.00	0.00	41.14	0.89	1.97	27.28
15/85	136.74	N.A.	N.A.	N.A.	0.76	5.30	25.67
0/100	180.39	N.A.	N.A.	N.A.	N.A.	N.A.	N.A.

[a] Ratio of recrystallization-exothermic and melting-endothermic heats: dimensionless. [b] Difference of endothermic and exothermic heats: J/g. [c] Endothermic heats by crystalline phase's weight fraction: J/g. [d] N.A. means "not available".

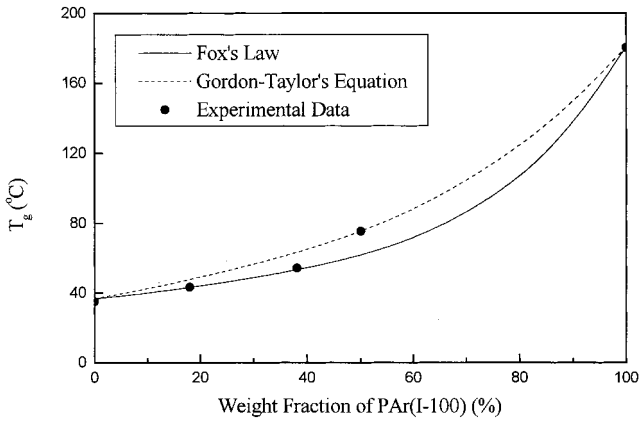

Figure 2. T_g versus composition as Fox and Gordon−Taylor equation: (—) Fox's law; (- - -) Gordon−Taylor's equation; (●) experimental data.

35, 50/50, and 0/100) were fitted by Fox's law. A value of 36.55 °C for the T_g of pure amorphous PBT was obtained from curve fitting by Fox's law. Then, this value of 36.55 °C was used in the Gordon−Taylor's equation. The best fit of eq 1 (solid line) and eq 2 (dash line) are shown in Figure 2. It was obvious that the T_g−composition variation could be well described by Fox's law and Gordon−Taylor's equation with $k = 0.36$. Although the Gordon−Taylor equation gave a satisfactory result for experimental data, nevertheless, it should be noted again that the T_g difference between PBT and PAr(I-100) was over 140 °C.

The overall thermal diagram of the PBT/PAr(I-100) system established by dynamic DSC analysis, was shown in Figure 1. For the blends with compositions of 100/0, 85/15, and 65/35, only one melting point (T_m) around 220 °C was found in each blend and it was the melting point of PBT crystals. However, two melting endotherms (around 220 and 280 °C) were found for the blends with compositions of 50/50 and 35/65. The lower melting point was the melting point of the PBT crystal and the higher melting point was the melting point of the PAr(I-100) crystal. For the blend of PBT/PAr(I-100) = 15/85, only one PAr(I-100) melting point was found. No melting point was found in the neat PAr(I-100). It should be mentioned that the as-prepared PAr(I-100) was completely amorphous. However, it could become semicrystalline after long-term annealing. The morphological transformation of PAr(I-100) before and after annealing could be observed in DSC (Figure 3-1a,b) and WAXD (Figure 3-2a,b) patterns. The crystallization rate of neat PAr(I-100) was very slow. However, it was significantly increased when the low-T_g component (PBT) was added (Figure 1). Since the dynamic DSC traces showed two distinct melting peaks for some blends, it could be concluded that PBT and PAr(I-100) crystals coexisted. Obviously, they did not form the cocrystals due to different chemical structures. In addition, they recrystallized at the different and well-separated temperature regimes. The recrystallization of PAr(I-100) occurred after the complete recrystallization of PBT. During the heating process, it was found that the recrystallization temperature of PBT increased with the increased PAr(I-100) content except for the neat PBT. This was primarily due to the increasing high-T_g component PAr(I-100) in the amorphous phase, causing the recrystallization shift to higher temperature. Although the crystal formed during the quenching process would increase the recrystallization temperature, the crystallinity of the blend during the quenching was decreased with the increasing PAr(I-100) contents (see Table 1). The decreasing of crystallinity should be favorable to the low-temperature recrystallization. Therefore, the effect of the high-T_g components dominated these behaviors. The most intriguing cases were the recrystallization temperature of PAr(I-100) in the 50/50, 35/65, and 15/85 composition ranges. The recrystallization temperature of PAr(I-100) should decrease with the addition of low-T_g components (PBT). However, the recrystallization temperature of PAr(I-100) in the 35/65 blend was slightly higher than observed in the 15/85 blend. It should be mentioned that the recrystallization of PAr(I-100) occurred immediately after the melting of PBT and might have partially overlap with the melting of PBT in the 35/65 blend. It was possible that the remixing of PBT and amorphous was not complete when the recrystallization of PAr(I-100) occurred. On the other hand, the crystallization rate of PAr(I-100) appeared to be significantly improved by the presence of a small amount of PBT (i.e., the 15/85 blend) in comparison with the neat PAr(I-100). It may be explained by the fact that the PBT increases the segmental mobility of PAr(I-100). Thus, it enhances the crystal growth of PAr(I-100).

Figure 4 shows the X-ray diffraction patterns of PBT, PBT/PAr(I-100) = 50/50 blend, and PAr(I-100) which isothermally crystallized at 200 or 250 °C. The X-ray diffraction pattern of neat PBT was similar to that reported by Tadokoro *et al.*[28] The pattern of neat PAr-(I-100) reconfirmed that it could crystallize and the crystallization rate was very slow. It was found that the 50/50 blend isothermally crystallized at 200 °C revealed several extra peaks in comparison with the neat PBT. Those peaks could be indexed by the neat PBT and PAr(I-100), respectively. It reconfirmed that the dual crystals could coexist in the 50/50 blend. Although the PBT/PAr(I-100) blend was miscible and the weak interaction existed between the unlike molecular group of PBT and PAr(I-100), the unit cells of PBT and PAr(I-100) crystals were never significantly modified by each other.

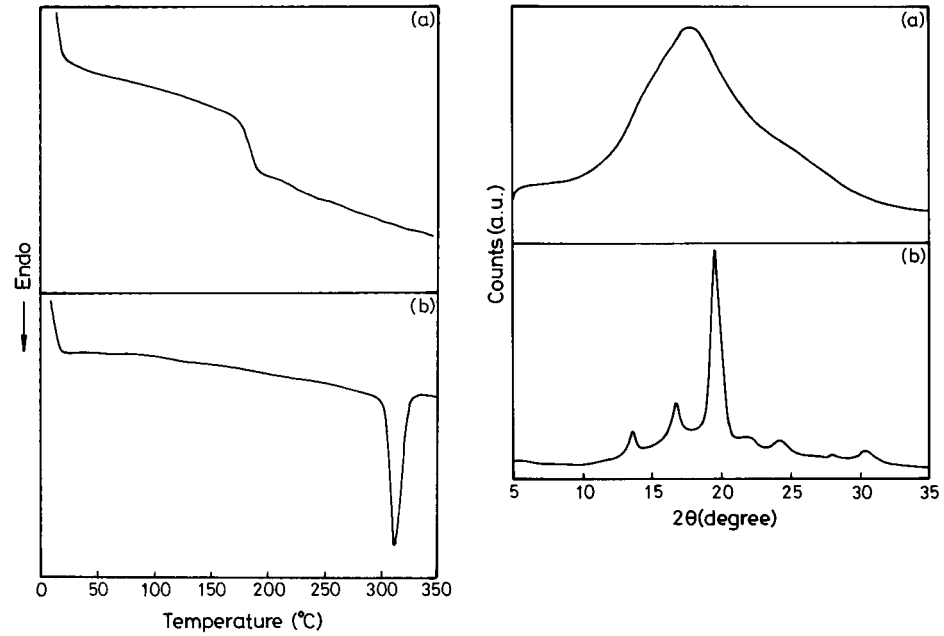

Figure 3. (Left) (a) DSC scan of amorphous PAr(I-100). (b) DSC scan of crystalline PAr(I-100). (right) (a) WAXD pattern of amorphous PAr(I-100). (b) WAXD pattern of crystalline PAr(I-100).

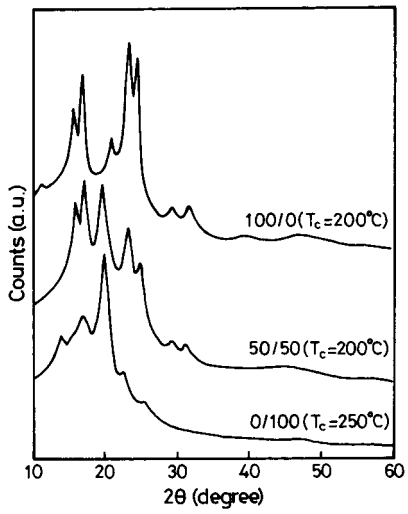

Figure 4. X-ray diffraction (WAXD) patterns of isothermally crystallized PBT/PAr(I-100) samples at different temperatures for 12 h.

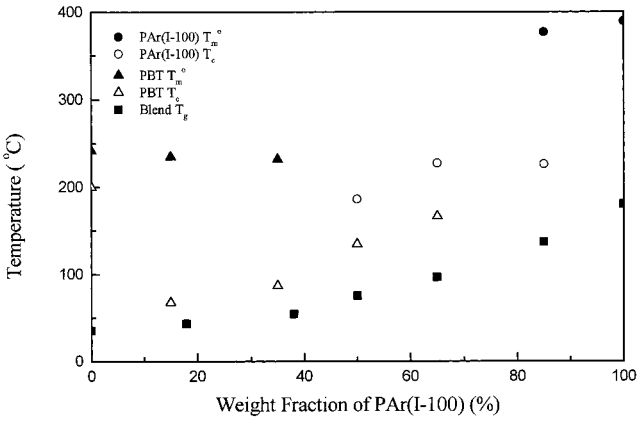

Figure 5. Thermodynamic behavior of PBT/PAr(I-100) blends: (●) PAr(I-100) T_m°; (○) PAr(I-100) T_c; (▲) PBT T_m°; (△) PBT T_c; (■) blend T_g.

In order to understand the effect of the PBT phase on the crystallization of PAr(I-100), and at the same time, the effect of the PAr(I-100) phase on the crystallization of PBT, we employed the ratio of exothermic and endothermic heats ($\Delta H_c/\Delta H_m$), the difference of endothermic and exothermic heats ($\Delta H_m - \Delta H_c$), and endothermic heats by the crystalline phase's weight fraction (ΔH_m/wt %) to determine the degree of suppression during the DSC second scanning. These results are summarized in Table 1.

First, from column five (ΔH_m/wt %) of Table 1, it was found that the 85/15 blend had the largest crystallinity of PBT. The result was similar to the results reported by Porter *et al.*[26] for PBT/PAr(I50-T50) blends. Comparing blends with the neat PBT, it was found from column three ($\Delta H_c/\Delta H_m$) of Table 1 that for PBT-rich blends (i.e., 85/15 and 65/35 blends), the crystallization of PBT on quenching was partially suppressed by the PAr(I-100) amorphous phase. Furthermore, the crystallization of PBT on quenching was almost completely suppressed by the PAr(I-100) when the weight fraction of PBT was less or equal to 50 wt %. With the increasing amount of PAr(I-100), the suppression effect on the crystallization of PBT was more pronounced. However, the melting points of PBT were nearly invariant up to 50/50 blend (Figure 1). On the other hand, the PAr(I-100) was strongly influenced by the presence of PBT in two aspects. The melting point of PAr(I-100) was significantly decreased by increasing the amount of PBT. This was not only the dilution effect of the PBT amorphous phase but also the suppression effect of the PBT crystalline phase. Also, the crystallization of PAr(I-100) was enhanced by addition of PBT. These behaviors were illustrated in Figure 5.

Before the discussion of isothermal crystallization behavior of blends, an important factor, transesterification, should be commented on here due to the long-time isothermal crystallization at high temperature. It was widely known that the interchange reaction commonly occurred in polyester blends. The interchange reaction in polyester blends involved acidolysis, alcoholysis, and direct transesterification. Devaux et al.[29]

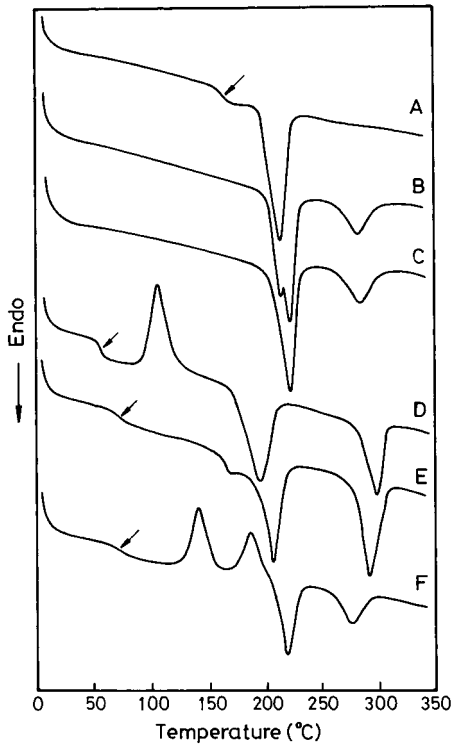

Figure 6. DSC traces of PBT/PAr(I-100) 50/50 blend of different heat-treatment conditions (see text). T_g is indicated by an arrow.

had reported that direct esterification was likely to occur in Bisphenol A polycarbonate (PC) with poly(ethylene terephthalate) (PET) and poly(butylene terephthalate) (PBT) blends. According to Kimura and Porter's[26] research, they concluded that transesterified PBT/PAr blends showed higher T_g's than the corresponding physical blends and also showed a marked T_m depression after treated in a vacuum oven at 250 °C for up to 16 h. To understand if a large degree of transesterification reaction did occur in our cases, the sample isothermally crystallized at 250 °C for 12 h was remelted again and quickly quenched in liquid nitrogen. Then the DSC scanning of the sample was carried out, and the result is shown as trace F of Figure 6. It was found that the DSC trace was similar to the case in Figure 1 for the 50/50 blend. The PAr(I-100) again recrystallized after the recrystallization of PBT. It indicated, at least, that the degree of transesterification was not large enough to significantly affect the crystallization behaviors of these blends.

Figure 6 shows the series of DSC scans of PBT/PAr(I-100) = 50/50 blends by different heat treatments. First, the trace A (crystallized at 150 °C for 12 h and then quenched to 0 °C followed by dynamic scanning up to 340 °C) exhibits only one endotherm of PBT. The blend could not form the PAr(I-100) crystal during the isothermal crystallization due to the low crystallization temperature. The composition of amorphous phase after the isothermal crystallization was shifted to 15/85 by weight fraction (ΔH_m = 37.08 J/g of PBT). The blend's T_g shifted to a higher temperature (162.91 °C) due to the change of amorphous composition and PBT crystalline phase. However, the 15/85 blend without previously formed PBT crystal (a little bit of PAr(I-100) previously formed) still could form the PAr(I-100) crystal during the DSC scanning (Figure 1). Hence, the PAr(I-100) crystal could not be formed due to not only the change of amorphous composition but also the previously formed PBT crystal phase. Furthermore, the blend could form the PAr(I-100) crystal if the sample was quickly jumped to 200 °C and maintained at that temperature for 12 h after the isothermal crystallization at 150 °C for 12 h (trace B). In trace B, the melting endotherm of PBT crystals was splitting into two peaks. The lower temperature was the melting point of a crystal formed during the crystallization at 150 °C. The higher temperature was the melting point of the crystal formed during the crystallization at 200 °C. The magnitude and position of the PAr(I-100) endotherm peak in trace B were comparable to those of the sample isothermally crystallized at 200 °C (Figure 6, trace C). Comparing traces A and B, it could be concluded that the PAr(I-100) could be formed even with the PBT crystal previously formed. However, the crystallization of PAr(I-100) was significantly affected not only by the change of amorphous composition but also the previously formed PBT crystals. The trace C (crystallized at 200 °C for 12 h and then quenched to 0 °C followed by dynamic scanning up to 340 °C) not only exhibited a PBT's endotherm but also a PAr(I-100)'s endotherm. Obviously, they could crystallize at the same temperature. The melting point of PBT isothermally crystallized at 200 °C was slightly higher than that of PBT crystallized at 150 °C due to the higher crystallization temperature. Trace D (crystallized at 250 °C for 12 h and then quenched to 0 °C followed by dynamic scanning up to 340 °C) also exhibited two melting peaks of PBT and PAr(I-100). Since the crystallization temperature was higher than the T_m of PBT, it could not to form any crystal of PBT during the isothermal crystallization at 250 °C. Obviously, the PBT crystal was formed during the quenching and heating processes. It meant that the PBT crystal could be formed even with PAr(I-100) crystal previously formed. It should be mentioned that the blend's T_g shifted to a lower temperature (54.48 °C), which is close to that of the composition 56/44 by weight fraction (Figure 2). If one considered the effect of previously formed PBT and PAr(I-100) crystals on the T_g, the amorphous phase should be richer in PBT content. However, the blend also could form the PBT crystals if the sample was quickly quenched to 150 °C and maintained at that temperature for 12 h after the isothermal crystallization at 250 °C for 12 h (trace E). It was clear that the melting peak of PBT compared with trace A was down to lower temperature due to the previously formed PAr(I-100) crystals [the amorphous phase should be PBT-rich after the crystallization of PAr(I-100)].

The equilibrium melting point was determined using Hoffman−Weeks[30] analysis. The equation was written in the following form

$$T_m = \frac{1}{\gamma}T_c + \left(1 + \frac{1}{\gamma}\right)T_m^\circ \qquad (3)$$

where T_m and T_m° are the experimental melting temperature and equilibrium melting temperature of PBT in the blend, respectively. γ is a proportional factor between the initial thickness of a chain-folded lamella, l_g*, and final lamellar thickness, l_c.

The equilibrium melting point, T_m°, was obtained from the extrapolation with the $T_m = T_c$ line. Figure 7 shows the Hoffman−Weeks plots for PBT and it PBT/PAr(I-100) blends, each piece of experimental data was obtained by isothermal crystallization for 12 h. Data

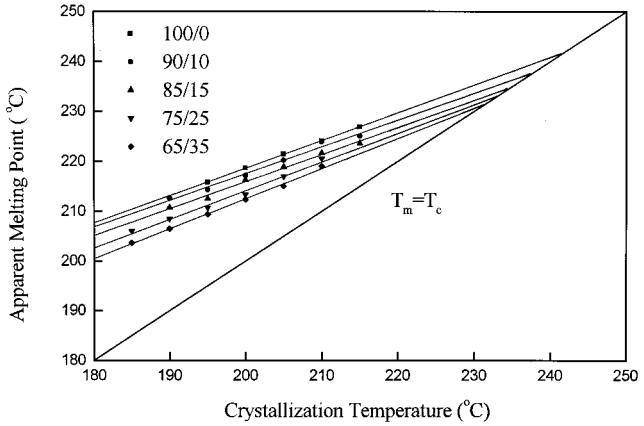

Figure 7. Hoffman−Weeks plots for PBT/PAr(I-100) blends: (■) 100/0; (●) 90/10; (▲) 85/15; (▼) 75/25; (◆) 65/35.

Table 2. Hoffman−Weeks Analysis for PBT/PAr(I-100) Blends

PBT/PAr(I-100)	equilibrium mp (°C)	thickening factor, γ
100/0	241.42	1.82
90/10	237.69	1.87
85/15	234.62	1.85
75/25	233.16	1.73
65/35	231.41	1.66

of 50/50 and 35/65 blends were dropped off due to the coexistence of PBT and PAr(I-100) crystals. Additional data of 90/10 and 75/25 blends were added. Thus, the samples used in Figure 7 contained the PBT crystals only. The values of T_m° and γ are listed in Table 2. The equilibrium melting point of PBT was reasonable in comparison with the data reported by Kimura *et al.*[26] (240 °C) and Cheng *et al.*[31] (245 °C) but was lower than that reported by Cebe and Huo[20] (249 °C). It was hard to make a direct comparison due to the different materials and blend compositions they used. We could find from Table 2 that the thickening ratio, γ, decreased with increasing PAr(I-100) content. This inferred that the PBT crystals became less stable due to the smaller lamellar thickness. However, the γ values of PBT/PAr-(I-100) 90/10 and 85/15 blend were greater than that of neat PBT. ,It might be helpful for PBT to become stable with a small amount of PAr(I-100).

The melting point depression of a crystalline phase with noncrystalline polymeric diluent in a miscible blend was derived by Nishi and Wang.[32] The equation could be written as

$$\frac{1}{T_m^\circ} - \frac{1}{T_m^{\circ\prime}} = \frac{-RV_2}{\Delta H_f^\circ V_1}\left[\frac{\ln \phi_2}{M_2} + \left(\frac{1}{M_2} - \frac{1}{M_1}\right)\phi_1\right] - \frac{RV_2}{\Delta H_f^\circ V_1}(\chi_{12}\phi_1^2) \quad (4)$$

where V is the molar volume of the polymer repeating unit, ϕ is the volume fraction of the component in the blend, ΔH_f° is the perfect crystal heat of fusion of the crystallizable polymer, M is the degree of polymerization, R is the universal gas constant, T_m° is the equilibrium melting point of pure crystalline polymer, $T_m^{\circ\prime}$ is the equilibrium melting point of a blend, and χ_{12} is the polymer/polymer interaction parameter. The subscripts 1 and 2 denote the amorphous and crystalline components, respectively. If the entropy of mixing could be negligible and the melting point depression was dominated by an enthalpic term, then the equation reduces to

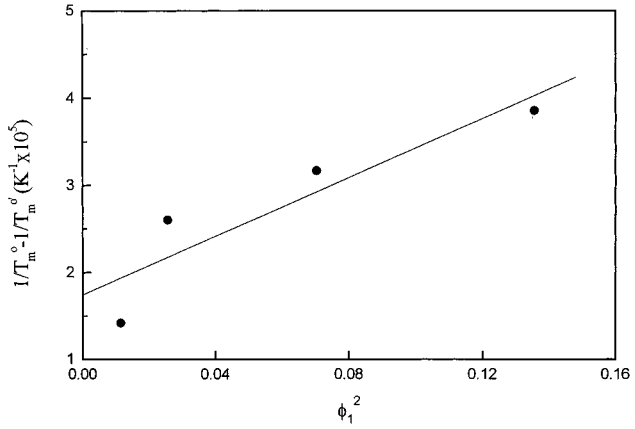

Figure 8. Flory−Huggin's interaction parameter calculated from the melting point depression of PBT.

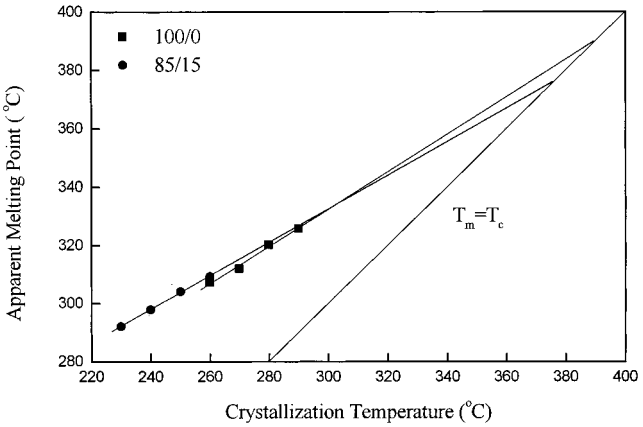

Figure 9. Hoffman−Weeks plots for PAr(I-100)/PBT blends: (■) 100/0; (●) 85/15.

$$\frac{1}{T_m^\circ} - \frac{1}{T_m^{\circ\prime}} = -\frac{RV_2}{\Delta H_f^\circ V_1}(\chi_{12}\phi_1^2) \quad (5)$$

It was well-known that experimental factors such as scanning rate, crystallization temperature range, and time of crystallization could affect the values obtained. Figure 8 shows the plot to obtain χ_{12} from eq 5. The following parameters are used: $\Delta H_f^\circ = 31.2$ kJ/mol of monomer (converted from 142 J/g),[27] $V_1 = 266.2$ cm^3/mol of monomer, and $V_2 = 129.6$ cm^3/mol of monomer. The molar volume of PAr(I-100) is assumed the same as that for PAr used by Kimura and Porter.[26] The interaction energy density, B, which is equal to $\chi_{12}RT/V_1$, would also be calculated. From the slope of the curve, it was found that $\chi_{12} = -1.3$ (at 241 °C) and ; $B = -5.0$ J/(cm^3 of PBT). It reconfirmed that the polymeric mixture was thermodynamically miscible in the melt.

A similar approach was also suitable for PAr(I-100) as a crystalline phase. Considering the ester-interchange reaction and the time required for the PAr(I-100) crystallization, two blends (100/0 and 85/15 blends) were chosen to achieve the equilibrium melting temperatures. Figure 9 showed the Hoffman−Weeks plot of PAr(I-100)/PBT blends. The result was listed in Table 3.

By comparison of Tables 2 with 3, it was found that the depression magnitude of PAr(I-100) was greater

Table 3. Hoffman−Weeks Analysis for PAr(I-100)/PBT Blends

PAr(I-100)/PBT	equilibrium mp (°C)	thickening factor, γ
100/0	389.40	1.56
85/15	376.72	1.74

than that of the PBT crystals. It inferred that the PAr-(I-100) molecule was more favorable to mix with the PBT. Unlike the PBT-rich blends, the plot has an intersection at $T_c = 304$ °C. In the meantime, the larger thickening factor of the 85/15 blend also implied that the existence of the PBT matrix could enhance the mobility of the crystallizable chain segments. Thus, it formed a thicker lamellae than the neat PAr(I-100). This influence of PBT crystallites on the crystallization of PAr(I-100) and the evidence of melting point depression for the 85/15 blend suggested the miscibility of PAr(I-100) and PBT in the melt.

Conclusion

The PBT/PAr(I-100) blend system exhibited a composition-dependent single T_g over the entire range of composition and an equilibrium melting point depression associated with a negative interaction parameter. It indicated that they were miscible in the whole range of composition. PBT and PAr(I-100) were able to form crystals at the same temperature simultaneously for the 50/50 blend. However, it did not form a cocrystal. Also, they could crystallize separately. It offered a chance to observe the effect of the crystal phase on the crystallization of the other components. The crystallization of PAr(I-100) was much faster when the PBT was added. It was due to the increasing segmental mobility by addition of low-T_g components. However, the previously formed crystallites of PBT in the blend suppressed the crystallization of PAr(I-100). It was due to the constraint of crystallites on the segmental mobility. The crystallization of PBT is slightly influenced by the presence of amorphous PAr(I-100) but severely suppressed by the presence of crystalline PAr(I-100).

Acknowledgment. The author expresses gratitude to the National Science Council for financial support under grant no. NSC 84-2216-E-002-017, and those who have contributed to this work are also acknowledged.

References and Notes

(1) Olabisi, O.; Robeson, L. M.; Shaw, M. T. *Polymer-Polymer Miscibility*; Academic Press: New York, 1979.
(2) Paul, D. R.; Barlow, J. W. *Macromol. Sci., Rev. Macromol. Chem.* **1980**, *18*, 109.
(3) Paul, D. R.; Barlow, J. W. *Polymer Science and Technology*; Plenum Press: New York, 1980; Vol. 11.
(4) Runt, J. P.; Martynowicz, L. M. *Muticomponent Polymer Materials*; American Chemical Society: Washington, 1986.
(5) Wu, W. B.; Chiu, W. Y.; Liau, W. B. *J. Appl. Polym. Sci.* **1997**, *64*, 411.
(6) Kyu, T.; Vadhar, P. *J. Appl. Polym. Sci.* **1986**, *32*, 5575.
(7) Natta, G.; Allegra, G.; Bassi, I. W.; Sianesi, D.; Caporiccio, G.; Torti, E. *J. Polym. Sci. A* **1965**, *3*, 4263.
(8) Natta, G.; Allegra, G.; Bassi, I. W.; Carlini, C.; Chiellini, E.; Montagnoli, G. *Macromolecules* **1969**, *2*, 311.
(9) Doll, W. W.; Lando, J. B. *Macromol. Sci. B* **1970**, *4*, 897.
(10) Harris, J. E.; Robeson, L. M. *J. Polym. Sci., Polym. Phys. Ed.* **1987**, *25*, 311.
(11) Avella, M.; Martuscelli, E. *Polymer* **1988**, *29*, 1731.
(12) Cimmino, S.; Martuscelli, E.; Silvestre, C. *Macromolecules* **1995**, *28*, 8065.
(13) Penning, J. P.; Manley, R. *Macromolecules* **1996**, *29*, 84.
(14) Avramova, N. *Polymer* **1995**, *36*, 801.
(15) Domines, J. D. *37th ANTEC of SPE* May 7−10, 1979, p 655.
(16) Freitag, D.; Reinking, K. *Kunststoffe* **1981**, *71* (1), 46.
(17) Sakata, H. *32nd ANTEC of SPE* April 13−16, 1974, p 459.
(18) Runt, J.; Miley, D. M.; Zhang, X.; Gallagher, K. P.; McFeaters, K.; Fishburn, J. *Macromolecules* **1992**, *25*, 1929.
(19) Runt, J.; Miley, D. M.; Zhang, X.; Gallagher, K. P. *Macromolecules* **1992**, *25*, 3902.
(20) Huo, P. P.; Cebe, P. *Macromolecules* **1993**, *26*, 3127.
(21) Borman, W. F. H. *J. Appl. Polym. Sci.* **1978**, *22*, 2119.
(22) Tseng, T. Y.; Chu, N. J.; Lee, Y. D. *J. Appl. Polym. Sci.* **1990**, *41*, 1651.
(23) Miley, D. M.; Runt, J. *Polymer* **1992**, *33*, 4643.
(24) Fox, T. G. *Bull. Am. Phys. Soc.*, **1956**, *1*, 123.
(25) Gordon, M.; Taylor, J. S. *J Appl. Chem.* **1952**, *2*, 493.
(26) Kimura, M.; Porter, R. S. *J. Polym. Sci., Polym. Phys. Ed.* **1983**, *21*, 367.
(27) Illers, K. H. *Colloid Polym. Sci.* **1980**, *258*, 117.
(28) Yokouchi, M.; Sakakibara, Y.; Chatani, Y.; Tadokoro, H. *Macromolecules* **1976**, *9*, 266.
(29) Devaux, J.; Godard, P.; Mercier, J. P. *J. Polym. Sci., Polym. Phys. Ed.* **1982**, *20*, 1875.
(30) Hoffman, J. D.; Weeks, J. J. *Res. Natl. Bur. Stand. A* **1962**, *66*, 13.
(31) Cheng, S. Z. D.; Pan, R.; Wunderlich, B. *Makromol. Chem.* **1988**, *189*, 2443.
(32) Nishi, T.; Wang, T. T. *Macromolecules* **1975**, *8*, 909.

MA980487K